Available online at www.sciencedirect.com

SCIENCE DIRECT®

Journal of Colloid and Interface Science 300 (2006) 298–303

Journal of
Colloid and
Interface Science

www.elsevier.com/locate/jcis

Two-dimensional "nano-ring and nano-crystal" morphologies in Langmuir monolayer of phthalocyaninato nickel complexes

Qingyun Liu [a], Hongguo Liu [a], Yongzhong Bian [a], Xueying Wang [a], Yanli Chen [a,b],
Jianzhuang Jiang [a,*], Xiyou Li [a,*]

[a] *Contribution from the Key Lab for Colloid and Interface Chemistry of Education Ministry, Department of Chemistry, Shandong University, Jinan 250100, China*
[b] *College of Chemistry and Chemical Engineering, Jinan University, Jinan 250022, China*

Received 1 February 2006; accepted 19 March 2006

Abstract

Three 1,8,15,22-tetrasubstituted phthalocyaninato nickel complexes Ni[Pc(α-OR)$_4$] [H_2Pc(α-OC$_5$H$_{11}$)$_4$ = 1,8,15,22-tetrakis(3-pentyloxy)-phthalocyanine; H_2Pc(α-OC$_7$H$_{15}$)$_4$ = 1,8,15,22-tetrakis(2,4-dimethyl-3-pentyloxy)phthalocyanine; H_2Pc(α-OC$_{10}$H$_7$)$_4$ = 1,8,15,22-tetrakis-(2-naphthyloxy)phthalocyanine] (**1**–**3**) have been prepared by treating the corresponding metal-free phthalocyanines H_2Pc(α-OR)$_4$ with Ni(acac)$_2$·2H$_2$O in refluxing n-pentanol. Structures of the Langmuir monolayers of these compounds at different temperature have been investigated. Compound **1** formed nano-ring structures with the outer diameter of 70–150 nm and inner diameter of 50 nm at 25.0 °C while **2** and **3** formed round particles. This difference can be ascribed to the different substituents at α position. The morphologies of the aggregates of **1** in monolayers have been found to change with temperature. Decreasing in temperature induced the formation of regular quadrate crystals. UV–vis absorption spectra revealed strong intermolecular interactions in the nano-ring aggregates. Polarized UV–vis absorption spectra suggest a titled orientation with respect to the surface of substrate for phthalocyanine macrocycles in the nano-ring aggregates.

Keywords: Nano-ring; Nano-crystal; Langmuir; Phthalocyaninato nickel

1. Introduction

The air–water interface provides an unique environment to assemble supramolecular structure where amphiphilic molecules can be orderly arranged and packed [1]. The construction of ordered supramolecular structure of phthalocyanines and metallo-phthalocyanines at the air–water interface have received much attention due to their potential applications as photoconductor, organic semiconductor, data storage material, and gas sensor [2–11]. Previous research results revealed that the use of phthalocyanine derivatives as building block to construct supramolecular structure at the air–water interface is very promising due to not only the strong π–π interaction between the macrocycles but also the tunable packing models of phthalocyanine rings by substitutions [12–14].

The packing of phthalocyanine derivatives at the air–water interface was dramatically affected by the substituents and their connecting position. A phthalocyanine with eight alkoxy groups at β position takes an "edge-on" conformation and forms one dimensional rod-like aggregates on water surface as revealed by Burghard [15] and Armstrong [16,17]. When the alkoxy groups were replaced by alkyl groups at the same position, the phthalocyanine ring took a different conformation with the phthalocyanine rings oriented parallel to the air–water interface, i.e., the so-called "face-on" conformation [18]. The aggregation behavior of asymmetrically octa-substituted phthalocyanine at α position with six hydrophobic alkoxy chains and two hydrophilic groups was found to depend on the chain length of the hydrophobic alkoxy chains. The compounds containing short alkoxy chains with carbon number less than (or equal to) six form J aggregates in the LB films [19,20], while the ones with longer alkoxy chains induce the formation of "herring-bond" aggregates [21–23]. All the results mentioned

---

[*] Corresponding authors. Fax: +86 531 88565211.
E-mail address: jzjiang@sdu.edu.cn (J. Jiang).

0021-9797/$ – see front matter © 2006 Elsevier Inc. All rights reserved.
doi:10.1016/j.jcis.2006.03.057

above indicate that the aggregation behavior of phthalocyanine derivatives at the air–water interface is sensitive to the substitution.

Tetra-substituted metallo-phthalocyanines at α position represent a very special group of compounds because of its unique C_{4h} symmetry [24,25]. This kind of compounds were synthesized by the tetramerization of corresponding α substituted phthalonitriles [26]. The introduction of a substituent with proper steric hindrance at α position can induce the isolation of isomer pure product in the tetramerization [27]. This is different from the tetra-β-substituted analogues which are usually a mixture of different isomers [28]. Special aggregation properties in solution have been revealed exclusively for these tetra-α-substituted compounds due to the special steric hindrance of the α-substituents [29]. However, the aggregation behavior of this kind of compound at the air–water interface is not yet studied. The investigation of aggregation behavior of these compounds at the air–water interface will give meaningful information on the relationship of the steric hindrance and the aggregate structure. Therefore we designed and prepared several tetra-α-substituted phthalocyaninato nickel(II) compounds and studied their aggregation behavior at the air–water interface in the present work.

2. Experimental

Complexes **1**, **2**, and **3** (Fig. 1) were synthesized according to literature procedure [25]. Chloroform (analytical grade) was purchased from Tianjin Chemical Reagent Co. and used as received without further purification.

Surface pressure–area (π–A) isotherms were recorded on a NIMA Langmuir–Blodgett 2000 trough (NIMA technology, UK). The surface pressure was measured using the Wilhelmy plate method with the accuracy of $\pm 0.1\ \mathrm{mN\,m^{-1}}$. Pure water (resistance: $18\ \mathrm{M\Omega\,cm^{-1}}$, pH: 6.4) was used as subphase. Dilute solutions of the complexes **1**, **2** and **3** in chloroform with the concentrations of 1.79×10^{-4}, 2.29×10^{-4} and $1.93 \times 10^{-4}\ \mathrm{mol\,L^{-1}}$, respectively, were spread onto the water surface. After 20 min for evaporating the solvent, π–A isotherms were obtained by compressing the barrier at a constant speed of $20\ \mathrm{cm^2\,min^{-1}}$. Monolayers and multilayers were deposited on hydrophobic quartz plates or glass substrates by using subphase lowering or vertical dipping method with a dipping speed of $7\ \mathrm{mm\,min^{-1}}$ while the surface pressure was kept at $20\ \mathrm{mN\,m^{-1}}$. The hydrophobic substrates were treated following the standard procedures of Hönig [30].

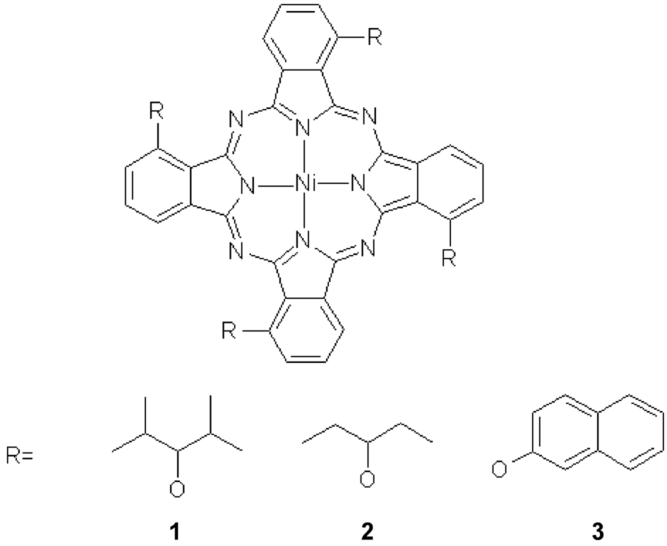

Fig. 1. Schematic molecular structure of phthalocyaninato nickel(II) complexes.

UV–vis absorption and polarized UV–vis absorption spectra were recorded on a U4100 spectrophotometer (Hitachi, Japan). For the polarized spectra, a dichroic sheet polarizer was placed in front of the LB films with s- and p-polarized lights, respectively. TEM images and selected-area electron diffraction were taken on a JEM-100CX II (JEOL Ltd., Japan) electron microscope operated at 100 kV.

3. Results and discussion

3.1. Surface pressure–area (π–A) isotherms at the air–water interface

π–A isotherms recorded at 25.0 °C for **1**, **2**, and **3** at the air–water interface are shown in Fig. 2. Stable monolayers are formed for all these three compounds with the collapsing pressures bigger than $30\ \mathrm{mN\,m^{-1}}$. The limiting molecular area (A_{limit}) obtained by extrapolating the condensed part to zero surface pressure, which corresponds to the hypothetical state of an uncompressed closed-packed layer where the molecules at the interface begin to interact with each other, is ca. 0.78, 0.76, and $0.63\ \mathrm{nm^2}$ for **1**, **2**, and **3** in its monolayer, respectively. For a flatly lying (face-on) phthalocyanine ring on water surface, the limiting molecular area would be expected to be ca. $1.74\ \mathrm{nm^2}$ based on the crystal structure. On the other hand, molecules standing perpendicularly (edge-on) to the water surface would yield the A_{limit} of ca. $0.65\ \mathrm{nm^2}$ [31]. The A_{limit} for these three complexes is close to the area occupied by an "edge-on" molecule, but much less than the area occupied by a "face-on" one, clearly suggesting either an "edge-on" conformation or the formation of multilayer films [32–35].

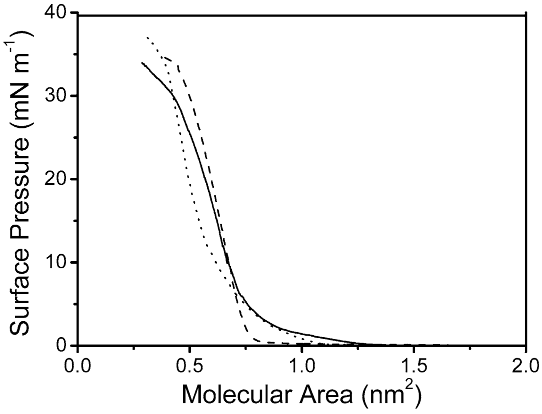

Fig. 2. π–A isotherms of **1** (—), **2** (- - -) and **3** (···) on water surface at 25.0 °C.

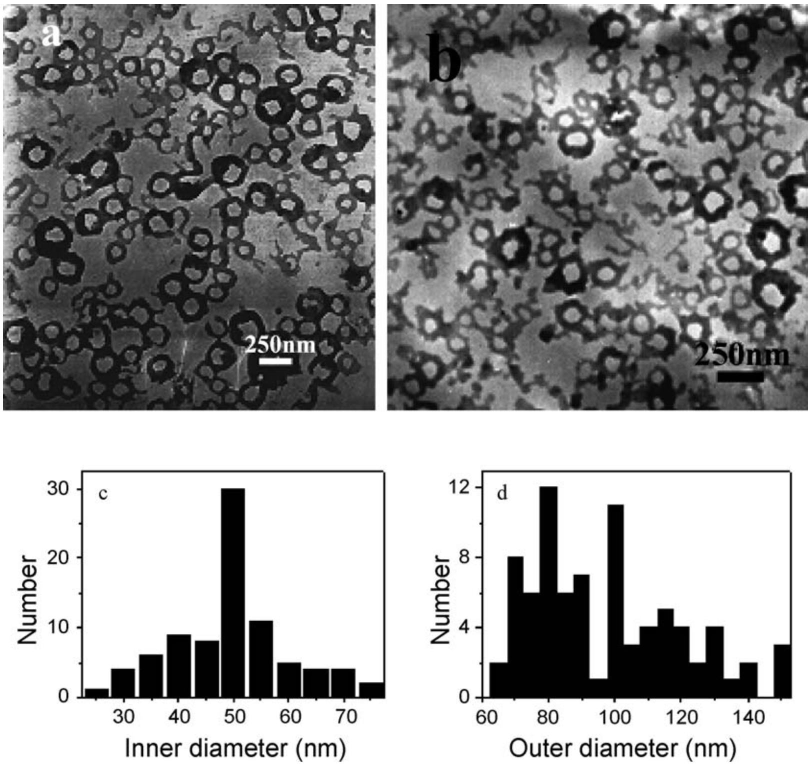

Fig. 3. TEM monolayer images of **1** at 25.0 °C with spreading concentrations of 1.79×10^{-4} mol L^{-1} (a) and 1.79×10^{-5} mol L^{-1} (b), and size distributions of inner (c) and outer (d) diameters corresponding to image (a).

3.2. *Temperature-dependent morphologies of monolayers of **1***

The monolayers at the air–water interface were kept at the target surface pressures (20 mN) for more than 30 min and then deposited to the 300-mesh copper grids covered with formvar by use of subphase lowering method in order to retain the monolayer morphologies. Fig. 3 shows the TEM images of the monolayers of **1** spread from the solution with different concentration at 25.0 °C. Regular rings and partial rings with a poorly defined periphery appear in the TEM images. The outer diameters of nano-rings range from ca. 70 to ca. 150 nm while the inner diameter of the ring is almost constant at ca. 50 nm. It can be seen from the size distribution curves that the inner diameter seems to be mono-dispersive, and the outer diameter is multi-dispersive, Fig. 3. This relates with the ring formation mechanism. Nanorings of porphyrin compounds have been fabricated from the organic or inorganic solvents [36–39]. An evaporation-driven solute transport mechanism was suggested for the nano-ring formation from the evaporation of organic solvents [38]. This mechanism is also considered to apply to the present system. It is worth noting that the nano-rings formed in our experiment is much smaller than the reported porphyrin nano-rings which range in diameter from 1 to several microns [37], while our phthalocyanine nano-rings have diameters in the range of 70–150 nm. The fabrication of porphyrin nano-rings was carried out on different solid substrate [36–39], while our phthalocyanine nano-rings are formed at the air–water interface. These differences might be responsible for the extremely small diameters of phthalocyanine nano-rings.

The formation of phthalocyanine nano-ring is not affected by the initial concentration of the spreading solution as indicated in Fig. 3b. This is different from the porphyrin case, the nano-rings of which dramatically depends on the initial concentration of the solution [36–39]. This can be ascribed to the very strong intermolecular interaction between phthalocyanine molecules, which drives the phthalocyanine molecules into aggregates even in a relative diluted solution. For instance, the monolayer was also deposited at a surface pressure of 5 mN m^{-1} and the similar nano-ring morphology with that of the film deposited at 20 mN m^{-1} was observed. This suggests that the nano-rings were formed before the compression process.

The monolayer shows different morphologies at different temperature, Fig. 4. When the temperature decreased from 25.0 to 23.0 °C, the irregular flake crystals appeared at the air–water interface, Fig. 4a. The continuous decrease in temperature caused the formation of relatively regular nanocrystals, Fig. 4b. Finally, well defined nanocrystals, i.e., quadrates, with the size of 70–100 nm were formed at 16.5 °C, Fig. 4c, which show clear ED patterns, inset of Fig. 4c.

In order to verify the influence of the molecular structure on the aggregation behavior, we also investigated the monolayer morphologies of **2** and **3**. The ring-like morphologies were not observed in the TEM images of their monolayers at the surface pressure of 20 mN, Fig. 5. What we found are usual round aggregates, similar to other monolayer aggregates of phthalocyanines formed at the air–water interface, indicating that the molecular structures or the substituents add great influence on the monolayer morphologies. The Langmuir monolayer morphologies of **2** and **3** were also investigated at the same tem-

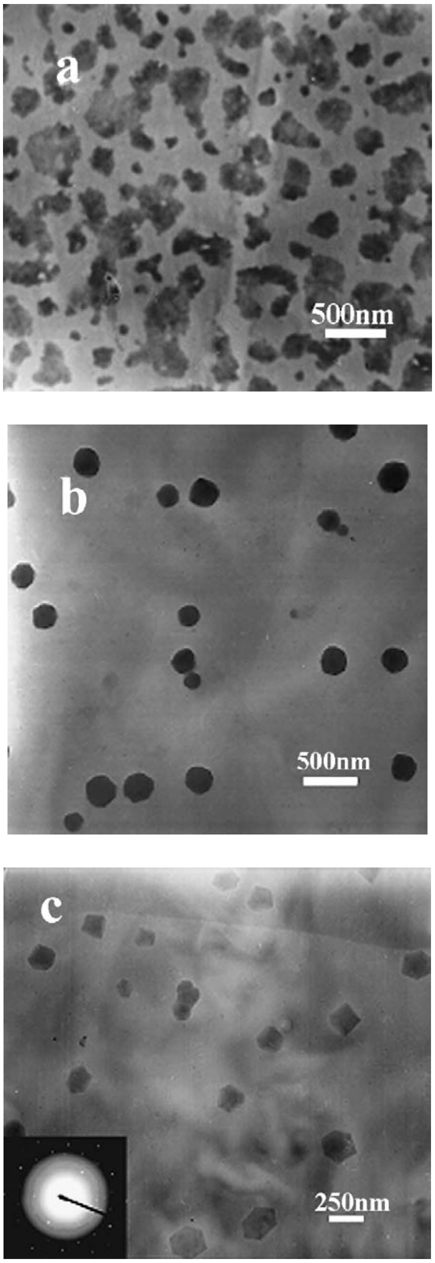

Fig. 4. The TEM nanocrystal images of **1** at various temperatures. (a) 23.0, (b) 19.5 and (c) 16.5 °C, respectively. The inset is electron diffraction pattern of regular nanocrystals.

perature range, 16.0–30 °C. It was found that the monolayer morphologies of **2** and **3** were not sensitive to the temperatures.

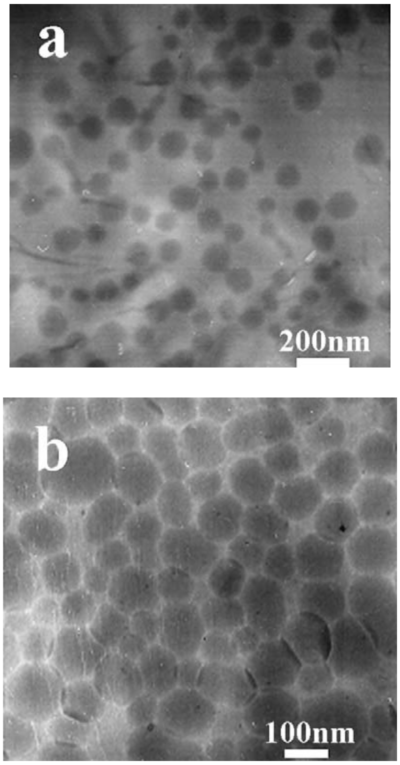

Fig. 5. TEM monolayer images of **2** (a) and **3** (b) deposited from the water surface at 25.0 °C.

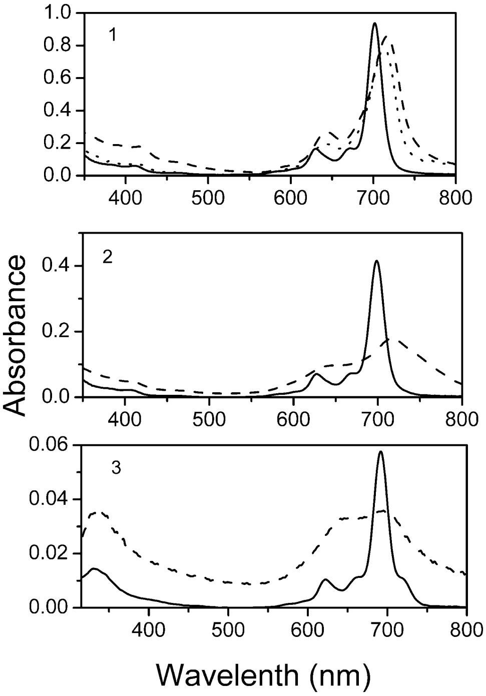

Fig. 6. UV–vis spectra of **1** (normalized at 708 nm), **2** and **3** in $CHCl_3$ (—), LB films at 25.0 °C (- - -) and nanocrystal films of **1** at 19.5 °C (···).

3.3. *UV–vis absorption and polarized UV–vis absorption*

Fig. 6 shows the UV–vis absorption spectra of **1**, **2**, and **3** in diluted chloroform solution and in LB films fabricated at 25.0 and 19.5 °C. The maximal characteristic Q bands corresponding to the π–π^* transitions of the phthalocyanine macrocycles of **1**, **2**, and **3** in dilute chloroform solution are at ca. 699, 702, and 692 nm, respectively. The characteristic Q bands of **1**, **2**, and **3** in the LB films deposited at 25 °C appear at ca. 717, 717, and 696 nm, red-shifted ca. 18, 15, and 4 nm, compared with that in dilute $CHCl_3$ solution, showing the formation of J-aggregates and closely packed structure according to Kasha's exciton coupling theory [40]. The broadening in the Q bands in LB films could be ascribed to the field effects of the closely compacted molecular assembly in LB films [41]. In addition,

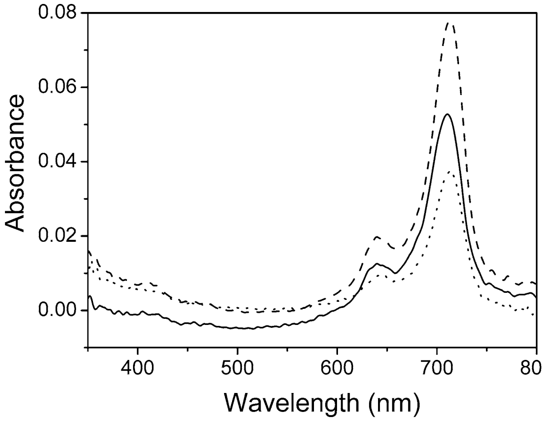

Fig. 7. UV–vis spectra of **1** nanocrystal films at 23.0 (—), 19.5 (- - -), and 16.5 °C (···).

LB films transferred at lower (5 $\mathrm{mN\,m^{-1}}$) or higher surface pressure (20 $\mathrm{mN\,m^{-1}}$) show similar UV–vis spectra, further revealing that the surface pressure does not give any influence on the aggregation of these molecules. This is also revealed by the TEM micrographs at different pressures.

Polarized UV–vis absorption spectra of LB films have been used in determining the orientation of phthalocyanine macrocycles in LB films. According to the reported method [42,43], the orientation angles of phthalocyanine macrocycles, θ, in LB films with respect to the substrate were obtained by using the dichroic ratios $D_\beta = A_\parallel / A_\perp$ ($\beta = 0°$ and $45°$) of the Q band and found to be 40° and 20° for the films of **1** and **2**, respectively, indicating that the macrocycles were tilted with respect to the substrate. The orientation of phthalocyanine derivatives at the air–water interface is controlled by the location and nature of the substituents grafted on the macrocycles. Because alkoxy chains grafted on the Pc ring are not polar enough to anchor the macrocycle parallel to the water surface. The macrocycles are thus tilted with respect to the water surface, and able to self-organize into columnar assemblies [44–46]. The big difference on the orientation angles of **1** and **2** suggests that the size of the substituents at α position significantly affect the conformation of phthalocyanines at the air–water interface, which is not observed for the β substituted phthalocyanines. The mean molecular area of these titled molecules in LB film was calculated based on the data of crystal structure and found that it is much bigger than the A_{limit} deduced from π–A isotherms [31]. This suggests the formation of multilayer films in the π–A isotherm studies. We cannot obtain the orientation angle for **3** due to the difficulty of depositing LB films. This can be ascribed to the very bad amphiphilic properties of this compound.

Monolayers of the nanocrystal of **1** formed at various temperatures were transferred to the hydrophilic quartz substrates and the UV–vis spectra were recorded, Fig. 7. The Q band appeared at about 710, 713, and 714.5 nm for the complex nanocrystals deposited at 23.0, 19.5, and 16.5 °C, respectively. The small red shift arises from the interaction between phthalocyanine macrocycles: The more regular the framework of the nanocrystals, the stronger the π-conjugated interaction, which then leads to bigger red shift of the Q band. The red shift of the Q band for the nanocrystal films of **1** was about 11 nm, which is a little bit smaller than that for the nano-ring film. As has been pointed out, the red shift of the Q band absorption is due to the π–π supramolecular interaction between two phthalocyanine macrocycles, it thus can be concluded that phthalocyanine interaction in the present nanocrystals is stronger than that in solution but slightly weaker than that in the nanoring films.

In a word, molecular structure and experimental conditions affect the interactions between molecules, resulting in the formation of different supramolecular structures that show distinct properties.

4. Conclusion

α substituted phthalocyanines aggregated at the air–water interface into nano-ring structure. This nano-ring structure is sensitive to the size and nature of the substituents and also to the environment temperature but not affected by the initial concentration of the solution. The properties of the supramolecular assembly of phthalocyanines can be tuned by changing the substituents and varying the experimental conditions. This is very useful in the construction of optical electronic devices.

Acknowledgments

Financial support from the Natural Science Foundation of China (Grant Nos. 20171028, 20325105, 20571049), National Ministry of Science and Technology of China (Grant No. 2001CB6105), Ministry of Education of China, and Shandong University is gratefully acknowledged.

References

[1] G.L. Ganis, Insoluble Monolayer at Liquid–Gas Interface, Wiley, New York, 1972.
[2] J. Jiang, K. Kasuga, D.P. Arnold, in: H.S. Nalwa (Ed.), Supramolecular Photo-Sensitive and Electro-Active Materials, Academic Press, New York, 2001, pp. 113–210.
[3] Z. Bao, A.J. Lovinger, A. Dodabalapur, Appl. Phys. Lett. 69 (1996) 3066–3068.
[4] R.D. Gould, Coord. Chem. Rev. 156 (1996) 237–274.
[5] D. Wöhrle, L. Kreienhoop, D. Schlettwein, in: C.C. Leznoff, A.B.P. Lever (Eds.), in: Phthalocyanines: Properties and Applications, vol. 1, VCH, New York, 1989, pp. 341–392.
[6] A.W. Snow, W.R. Barger, in: C.C. Leznoff, A.B.P. Lever (Eds.), in: Phthalocyanines: Properties and Applications, vol. 1, VCH, New York, 1989, pp. 345–392.
[7] Y. Chen, W. Su, M. Bai, J. Jiang, X. Li, Y. Liu, L. Wang, S. Wang, J. Am. Chem. Soc. 127 (2005) 15700–15701.
[8] J. Zhang, J. Wang, H. Wang, D. Yan, Appl. Phys. Lett. 84 (2004) 142–144.
[9] R. Zeis, T. Siegrist, Ch. Kloc, Appl. Phys. Lett. 86 (2005) 22103-1–22103-3.
[10] M. Erik, M. Taniguchi, T. Kawai, Appl. Phys. Lett. 86 (2005) 143513-1–143513-3.
[11] D. Xie, J. Jiang, Z. Wu, Y. Li, Sens. Actuators B 77 (2001) 260–263.
[12] J.R. Fryer, R.A. Hann, B.L. Eyres, Nature (1985) 382–384.
[13] A.W. Snow, N.L. Jarvis, J. Am. Chem. Soc. 106 (1984) 4706–4711.
[14] M.J. Cook, I. Chambrier, in: K.M. Kadish, K.M. Smith, R. Guilard (Eds.), in: The Porphyrin Handbook, vol. 17, Elsevier Science, New York, 2003, pp. 77–79, and the reference therein.

[15] M. Burghard, M. Schmelzer, S. Roth, P. Haisch, M. Hanack, Langmuir 10 (1994) 4265–4269.

[16] P. Smolenyak, R. Peterson, K. Nebesny, M. Torker, D.F. O'Brien, N.R. Armstrong, J. Am. Chem. Soc. 121 (1999) 8628–8636.

[17] R.A.P. Zangmeister, P.E. Smolenyak, A.S. Drager, D.F. O'Brien, N.R. Armstrong, Langmuir 17 (2001) 7071–7078.

[18] H. Nakahara, K. Fukuda, K. Kitahara, H. Nishi, Thin Solid Films 178 (1989) 361–366.

[19] M.J. Cook, J. McMurdo, D.A. Miles, R.H. Pounter, J.M. Simmons, S.D. Haslam, R.M. Richardson, K. Welford, J. Mater. Chem. 4 (1994) 1205–1213.

[20] A.K. Ray, A.V. Nabok, A.K. Hassan, O. Omar, R. Taylor, K.J. Cook, Philos. Mag. B 78 (1998) 53–64.

[21] M.J. Cook, M.F. Daniel, K.J. Harrison, N.B. McKeown, A.J. Thomson, J. Chem. Soc., Chem. Commun. 15 (1987) 1148–1150.

[22] N.B. McKeown, M.J. Cook, A.J. Thomson, K.J. Harrison, M.F. Daniel, R.M. Richardson, S.J. Roser, Thin Solid Films 159 (1988) 469–478.

[23] M.J. Cook, Int. J. Electronics 76 (1994) 727–761.

[24] Y.Z. Bian, R.M. Wang, J.Z. Jiang, C.H. Lee, J.Z. Wang, D.K.P. Ng, Chem. Commun. (2003) 1194–1195.

[25] W. Liu, C. Lee, H. Li, C. Lam, J. Wang, T.C.W. Mak, D.K.P. Ng, Chem. Commun. (2002) 628–629.

[26] K. Kasuga, M. Kawashima, K. Asano, T. Sugimori, K. Abe, T. Kikkawa, T. Fujiwara, Chem. Lett. (1996) 867–868.

[27] C. Rager, G. Schmid, M. Hanack, Chem. Eur. J. 5 (1999) 280–288.

[28] C.C. Leznoff, in: C.C. Lezonff, A.B.P. Lever (Eds.), in: Phthalocyanines Properties and Applications, vol. 1, VCH, New York, 1989, pp. 4–54.

[29] K. Kasuga, N. Matsuura, K. Inoue, M. Handa, T. Sugimori, K. Isa, M. Nakata, Chem. Lett. (2002) 352–353.

[30] E.P. Honig, J.H.T. Hengst, D.D. Engelsen, J. Colloid Interface Sci. 45 (1973) 92–102.

[31] Crystal data of **1**: Monoclinic, unit cell: $a = 15.8081$, $b = 8.8351$, $c = 21.5308$, $\alpha = 90.000$, $\beta = 99.917$, $\gamma = 90.000$.

[32] Y. Matsuzawa, T. Seki, K. Ichimura, Langmuir 14 (1998) 683–689.

[33] D.J. Qian, C. Nakamura, J. Miyake, Thin Solid Films 397 (2001) 266–275.

[34] H. Chou, C. Chen, K.F. Stork, P.W. Bohn, K.S. Suslick, J. Phys. Chem. 98 (1994) 383–385.

[35] Q. Lu, Y. Luo, L. Li, M. Liu, Langmuir 19 (2003) 285–291.

[36] S.C. Doan, S. Shanmugham, D.E. Aston, J.L. McHale, J. Am. Chem. Soc. 127 (2005) 5885–5892.

[37] A.P.H.J. Schenning, F.B.G. Benneker, H.P.M. Geurts, X.Y. Liu, R.J.M. Nolte, J. Am. Chem. Soc. 118 (1996) 8549–8552.

[38] J. Hofkens, L. Latterini, P. Vanoppen, H. Faes, K. Jeuris, S.D. Feyter, J. Kerimo, P.F. Barbara, F.C.D. Schryver, L.E. Rowan, R.J.M. Nolte, J. Phys. Chem. B 101 (1997) 10588–10598.

[39] L. Latterini, R. Blossey, J. Hofkens, P. Vanoppen, F.C.D. Schryver, A.E. Rowan, R.J.M. Nolte, Langmuir 15 (1999) 3582–3588.

[40] M. Kasha, H.R. Rawls, M.A. El-Bayoumi, Pure Appl. Chem. 11 (1965) 371–392.

[41] Y.L. Chen, H.G. Liu, N. Pan, J. Jiang, Thin Solid Film 460 (2004) 279–285.

[42] M. Yoneyama, M. Sugi, M. Saito, K. Ikegami, S. Kuroda, S. Iizima, Jpn. J. Appl. Phys. 1 (1986) 961–965.

[43] X.M. Ding, H.J. Xu, L. Zhang, D. Jiang, A. Lu, Thin Solid Films 340 (1999) 271–273.

[44] S. Palacin, Adv. Colloid Interface Sci. 87 (2000) 165–181.

[45] H. Itoh, T. Koyama, K. Hanabusa, E. Masuda, H. Shirai, T. Hayakawa, J. Chem. Soc., Dalton Trans. (1989) 1543–1546.

[46] K. Ogawa, S. Kinoshita, H. Yonehara, H. Nakahara, K. Fukuda, J. Chem. Soc., Chem. Commun. (1989) 477–479.